

# Towards a Propagation Model for Wireless Biomedical Applications

**S.K.S. Gupta, S. Lalwani**

Department of Computer Sc.& Engg.  
Arizona State University  
Tempe, AZ 85287  
sandeep.gupta@asu.edu

**Y. Prakash, E. Elsharawy**

Department of Electrical Engg.  
Arizona State University  
Tempe, AZ 85287  
yashwanth\_p@asu.edu

**L. Schwiebert**

Department of Computer Sc.  
Wayne State University  
Detroit, MI 48202  
loren@cs.wayne.edu

**Abstract**— Propagation model plays a very important role in designing wireless communication systems. Current advances in semiconductor technology has made it possible to implant a network of bio-sensors inside the human body for health monitoring purposes [12], [14], [8]. For wireless communication inside the human body, the tissue medium acts as a channel through which the information is sent as electromagnetic (EM) radio frequency (RF) waves. A propagation model is necessary to determine the losses involved in the form of absorption of EM wave power by the tissue. Absorption of EM waves by the tissue body, which consists of mostly saline water, accounts for a major portion of the propagation loss. In this paper we present a propagation loss model (PMBA) for homogeneous tissue bodies. We have verified the model for the frequency range of our interest (900MHz to 3GHz) using a 3D EM Simulation Software, HFSS™, and experimental measurements using saturated salt water.

## I. INTRODUCTION

Many propagation models like 2-ray model, Okumura model [1] have been developed for wireless applications with air as the medium, which consider the losses in the form of fading due to multipath, reflection, diffraction, and scattering. However a channel model for biomedical applications involving wireless communication between the implanted sensors inside the body has not been developed. When EM RF waves propagate in freespace, the power received decreases at a rate of  $(1/d)^n$  [1],  $n$  being the coefficient of pathloss. Other kinds of losses would be fading of signals due to multipath propagation. However, for propagation of EM waves in a lossy medium like human tissue, the losses would be mainly due to absorption of power in the tissue, which is dissipated as heat. As the tissue medium is lossy and mostly consists of water, the EM waves are attenuated considerably before they reach the receiver.

The *Specific Absorption Rate* (SAR) is useful in determining the amount of power lost due to heat dissipation. SAR is defined as power absorbed per unit mass of the tissue [4]. SAR is a standard measure of how much power is absorbed in the tissue and depends upon  $E$ - and  $H$ -field strengths. By determining the average SAR over the entire mass of the tissue between the transmitter and the receiver, we are able to compute the total power lost. SAR in the near field of the transmitting antenna depends mainly on the  $H$ -field, whereas the SAR in the far field

of the transmitting antenna depends mainly on the  $E$ -field. We use Maxwell's  $E$ - and  $H$ -fields equations for lossy medium to obtain the average SAR of the medium between the transmitting and the receiving antenna in the far field and near field, respectively. Thus the propagation loss in the channel is modeled mainly by considering the power absorbed by the tissue medium.

## II. RELATED WORK

Little research has been done in the area of developing propagation models for RF Communication inside human body. However, there has been considerable research going on in the field of measurement of power absorption in human tissues, calculation of SAR, and specification of safe absorption rates. This paves the way for the development of a propagation model for Biomedical applications.

Pandit et al. [13] have used a finite-difference time-domain (FDTD) method to calculate the power deposition in a human head as measured by the SAR in W/Kg. However the actual model that describes the relation between power received and the distance from the source inside a human body has not been developed.

Kuster and Balzano [6] have studied the energy absorption mechanism in the close near-field region of a dipole antenna by numerical simulations for frequencies above 300MHz. They have found that the SAR is mainly proportional to the square of the  $H$ -field, which implies that, in the close near-field regions, the peak SAR is related to the antenna current and not the input power. We make use of the approximate formula developed by them for estimating the average SAR in the near-field region.

The NCRP report [4] has a detailed description of procedures for evaluation of RF exposure, instruments used, and measurement techniques. The report also explains the SAR characteristics. The SAR equation for estimating power absorbed in the far-field region in PMBA is obtained from this report.

## III. SYSTEM MODEL

Applications like [8] and [7], involve wireless communications between implanted biosensor nodes inside human body.

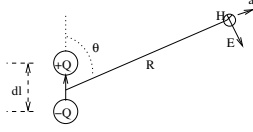


Fig. 1. A Hertzian Dipole [3]

These nodes exchange data among themselves and also with the basestation. In general, the system model consists of numerous biosensor nodes placed inside the various parts of the human body surrounded by tissues. In particular, for the development of this model, we consider only one transmitting and one receiving antenna separated by a distance  $d$ . An elemental short dipole (dipole length  $\ll$  wavelength) in a lossy human tissue medium is considered for this purpose [3] and is shown in Fig. 1. A small area of tissue surrounding the antenna is considered for our analysis. Thus we can safely assume the human tissue under consideration to be a homogeneous medium with no sharp edges, no rough surfaces and having uniform electric and magnetic properties. The received power is assumed to be due only to the power from the transmitter and not from any other source. The space around the radiating antenna is divided into near field and far field regions as shown in Fig. 2. The region of space immediately surrounding the antenna is known as the near field region. The extent of the near field in the case of short dipoles is given by  $d_0 = \lambda/2\pi$ , where  $\lambda$  is the wavelength [5]. In the near field, the  $E$ - and  $H$ -field strengths vary rapidly with the distance from the antenna. The far field is the entire region beyond the near field. In the far field region, the  $E$ - and  $H$ -field exhibit a plane wave behavior. Power absorbed between the transmitting and receiving antennas can be considered as the sum of power absorbed in near field ( $P_{NF}$ ) and far field ( $P_{FF}$ ) regions. The total power absorbed between the two antennas is computed by numerical integration and is explained in the next section.

#### IV. DERIVATION

Consider an elemental oscillating electric dipole in a lossy medium of conductivity  $\sigma$  (S/m), permittivity  $\epsilon$  (F/m), permeability  $\mu$  (H/m), complex propagation constant  $\gamma$ , complex intrinsic impedance  $\eta = \frac{\gamma}{\sigma + j\omega\epsilon}$  [3] at frequency  $\omega$ , as shown in Fig. 1. The dipole consists of a short conducting wire of length  $dl$ , terminated in two small conductive spheres or disks. Assume that the current  $I$  is uniform and varies sinusoidally with time [3]. The electromagnetic field at a distance ' $R$ ' for an Hertzian dipole is derived from the vector potential  $A$ , given by [3],

$$A = \mathbf{a}_z \frac{\mu I dl e^{-\gamma R}}{4\pi R} = \mathbf{a}_z A_z,$$

where  $\mathbf{a}_z$  is the unit vector in the  $z$ -direction,  $\gamma$  is the propagation constant, given by  $\gamma = \alpha + j\beta$ ; attenuation constant  $\alpha$  and

phase constant  $\beta$  is given as [3],

$$\alpha = \omega \sqrt{\frac{\mu\epsilon}{2}} \left[ \sqrt{1 + \left(\frac{\sigma}{\omega\epsilon}\right)^2} - 1 \right]^{1/2} \quad (\text{Neper/m})$$

$$\beta = \omega \sqrt{\frac{\mu\epsilon}{2}} \left[ \sqrt{1 + \left(\frac{\sigma}{\omega\epsilon}\right)^2} + 1 \right]^{1/2} \quad (\text{rad/m})$$

Spherical components of  $A$  (i.e.,  $a_R A_R + a_\theta A_\theta + a_\phi A_\phi$ ) are given by  $A_R = A_z \cos \theta$ ,  $A_\theta = -A_z \sin \theta$  and  $A_\phi = 0$ . The magnetic field intensity  $H$  and the electric field intensity  $E$  is given by [3],

$$H = \frac{1}{\mu} (\nabla \times A) = a_\phi \frac{1}{\mu R} \left[ \frac{\partial}{\partial R} (R A_\theta) - \frac{\partial}{\partial \theta} A_R \right],$$

$$E = \frac{1}{\sigma + j\omega\epsilon} (\nabla \times H) \\ = \frac{1}{\sigma + j\omega\epsilon} \left[ a_R \frac{1}{R \sin \theta} \frac{\partial}{\partial \theta} (H_\phi \sin \theta) - a_\theta \frac{1}{R} \frac{\partial}{\partial R} (R H_\phi) \right]$$

Solving the above magnetic and electric field equations for lossy medium and expressing in terms of complex impedance  $\eta$  we get:

$$E_R = \eta \frac{2I dl \cos \theta}{4\pi} e^{-\gamma R} \left( \frac{1}{\gamma R^3} + \frac{1}{R^2} \right) \quad (1)$$

$$E_\theta = \eta \frac{I dl \sin \theta}{4\pi} e^{-\gamma R} \left( \frac{1}{\gamma R^3} + \frac{1}{R^2} + \frac{\gamma}{R} \right) \quad (2)$$

$$H_\phi = \frac{I dl \sin \theta}{4\pi} e^{-\gamma R} \left( \frac{1}{R^2} + \frac{\gamma}{R} \right) \quad (3)$$

##### A. Power absorbed in the Near Field

The SAR in the near field is given by [6],

$$SAR = \frac{\sigma}{\rho} \frac{\mu\omega}{\sqrt{\sigma^2 + \epsilon^2\omega^2}} (1 + c_{corr}\tau)^2 H_{rms}^2 \text{ watts/Kg}$$

where  $\rho$  is the density of the medium and  $c_{corr}$  is the correction factor to take into account the changed reflection properties for small distances  $R$  of the antenna from the scatterer. Since we assume both the transmitting and receiving antennae are in a same homogeneous medium, the plane wave reflection coefficient  $\tau$  is zero. By substituting  $\tau = 0$  and RMS value of the  $H$ -field, the above equation reduces to

$$SAR = \frac{\sigma}{\rho} \frac{\mu\omega}{\sqrt{\sigma^2 + \epsilon^2\omega^2}} \left( \frac{I dl \sin \theta}{4\pi} e^{-\alpha R} \left( \frac{1}{R^2} + \frac{|\gamma|}{R} \right) \right)^2,$$

which gives the value of SAR at a point at distance ' $R$ ' and angle ' $\theta$ ' from the dipole. Power at infinitely small volume ( $dV = R^2 \sin \theta dR d\theta d\phi$ ) is

$$\Delta P = SAR \times \Delta mass = SAR \times \rho \times dV \quad (4)$$

The power absorbed in the near field of the lossy tissue can be obtained by computing the average SAR over the entire tissue

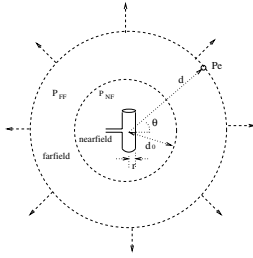


Fig. 2. Field regions around a Hertzian Dipole

mass in the near field, which is obtained by integrating  $\Delta P$  over the entire mass in the near field region, i.e., from the surface of the antenna ( $R = r$ ) to the end of the near-field region ( $R = d_0$ )

$$\begin{aligned}
 P_{NF} &= \int_{R=r}^{d_0} \int_{\theta=0}^{\pi} \int_{\phi=0}^{2\pi} \Delta P \\
 &= \sigma \frac{\mu\omega}{\sqrt{\sigma^2 + \epsilon^2\omega^2}} \left( \frac{I dl}{4\pi} \right)^2 \int_{R=r}^{d_0} \int_{\theta=0}^{\pi} \int_{\phi=0}^{2\pi} R^2 \sin^3 \theta \\
 &\quad \times e^{-2\alpha R} \left( \frac{1}{R^4} + \frac{|\gamma|^2}{R^2} + \frac{2|\gamma|}{R^3} \right) dR d\theta d\phi
 \end{aligned}$$

Solving by numerical integration and writing  $\frac{1}{\sqrt{\sigma^2 + \epsilon^2\omega^2}}$  as  $|\eta|/|\gamma|$ ,

$$\begin{aligned}
 P_{NF} &= \sigma\mu\omega \frac{|\eta|}{|\gamma|} \frac{I^2 dl^2}{6\pi} [A + B + C], \text{ where} \quad (5) \\
 A &= e^{-2\alpha r} \left( \frac{|\gamma|^2}{2\alpha} + \frac{d_0 - r}{4r^2} + \frac{|\gamma|(d_0 - r)}{2r} \right), \\
 B &= e^{-2\alpha d_0} \left( \frac{-|\gamma|^2}{2\alpha} + \frac{d_0 - r}{4d_0^2} + \frac{|\gamma|(d_0 - r)}{2d_0} \right), \text{ and} \\
 C &= e^{-\alpha(d_0+r)} \left( \frac{2(d_0 - r)}{(d_0 + r)^2} + \frac{2|\gamma|(d_0 - r)}{(d_0 + r)} \right)
 \end{aligned}$$

The antenna dimensions depend on the wavelength of the wave in the medium given by  $\lambda_m = \frac{2\pi}{\beta}$  [3].

### B. Power absorbed in the Far Field

Neglecting  $\frac{1}{R^2}, \frac{1}{R^3}, \dots$  terms from field equations (1)-(3) for the far field, we have

$$\begin{aligned}
 E_R &= 0, \quad E_\theta = \eta \frac{I dl \sin \theta}{4\pi} e^{-\gamma R} \left( \frac{\gamma}{R} \right) \\
 H_\phi &= \frac{I dl \sin \theta}{4\pi} e^{-\gamma R} \left( \frac{\gamma}{R} \right)
 \end{aligned}$$

In the far field the specific absorption rate depends only on the  $E_{rms}$  value which is given by [4],

$$\begin{aligned}
 SAR &= \frac{\sigma}{\rho} E_{rms}^2 \text{ watts/Kg} \\
 &= \frac{\sigma}{\rho} \left( |\eta| |\gamma| \frac{I dl \sin \theta}{4\pi R} e^{-\alpha R} \right)^2
 \end{aligned}$$

The power absorbed in the infinitely small volume ( $dV = R^2 \sin \theta dR d\theta d\phi$ ) in the far field, at a distance  $R$  and angle  $\theta$  from the dipole can again be obtained from (4),

$$\Delta P = \sigma \left( |\eta| |\gamma| \frac{I dl}{4\pi} \right)^2 \sin^3 \theta e^{-2\alpha R} dR d\theta d\phi$$

The total power absorbed in the far field of the lossy tissue between the source and destination antennas can be obtained by computing the average SAR over the entire tissue mass in the far field from distance  $d_0$  to  $d$  ( $d_0$  is the point where the far field starts). This is obtained by integrating  $\Delta P$  over the mass in the far field between the two antennas.

$$\begin{aligned}
 P_{FF} &= \int_{R=d_0}^d \int_{\theta=0}^{\pi} \int_{\phi=0}^{2\pi} \Delta P \\
 &= \sigma |\eta|^2 |\gamma|^2 \frac{I^2 dl^2}{12\pi\alpha} (e^{-2\alpha d_0} - e^{-2\alpha d}) \quad (6)
 \end{aligned}$$

### C. Power received

The effective radiated power (ERP) is obtained by subtracting the loss in the near field ( $P_{NF}$ ) and far field ( $P_{FF}$  between the transmitting and receiving antennas) from the transmitted power  $P_T$  (i.e.,  $(P_T - P_{Loss})G_t$ ), where  $P_{Loss} = P_{NF} + P_{FF}$  is obtained from (5) and (6). The power density ( $P_e$ , Power per unit area) at a distance 'd' is different in near field and far field regions.

1)  $P_R$  in the Near Field: There is no general formula for the estimation of field strength in the near field zone [5]. Only measurements can provide a simple means of field evaluation. However, reasonable calculations can be made for antennas like dipole or monopole. When the receiving antenna is in the near field region of the transmitting antenna, the power density does not necessarily depend on the distance from the antenna, but varies rapidly with distance, and may exhibit oscillatory behavior. The magnitude of on-axis (main beam) power density varies according to the location in the near field and its maximum value is approximated by [10]  $P_e = 16\delta P/\pi L^2$ , where  $L$  is the largest dimension of the antenna,  $P$  is  $P_T - P_{NF}$ , and  $\delta$  is the aperture efficiency (typically 0.5-0.75) [10]. It can be approximated as  $\delta = A_e/A$  ( $A_e$  is the effective aperture and  $A$  is the physical area of the antenna). The power received by the receiving antenna in the near field can be approximated by

$$P_R = P_e A_e = \frac{16\delta(P_T - P_{NF})}{\pi L^2} A_e$$

2)  $P_R$  in the Far Field: On the other hand when the receiving antenna is in the far field region of the transmitting antenna, the power density is dependent on the distance  $d$  and is given by

$$P_e = \frac{(P_T - P_{Loss})}{4\pi d^2} G_t$$

The power received by the receiving antenna in the far field is  $P_R = P_e A_e$ , where the receiving antenna aperture  $A_e$  is given

by [2] as  $A_e = \frac{\lambda^2}{4\pi} G_t G_r$ . Here,  $G_t$  and  $G_r$  are the gain of the transmitting and receiving antenna, respectively. Thus the received power is

$$P_R = \frac{(P_T - P_{NF} - P_{FF})\lambda^2}{(4\pi d)^2} G_t G_r$$

And a total phase change of  $e^{-j\beta}$  is involved during the propagation of the wave. Thus, PMBA can be used for calculating the propagation loss using the two equations (5) and (6).

## V. VALIDATION OF PMBA

### A. HFSS

We have simulated the tissue channel characteristics, with the help of HFSS (3D EM Simulation Software for RF by AN-SOFT Inc.). Two probes, each of length 20mm and diameter 1mm are defined. These dimensions are chosen in accordance with the probe dimensions that are used for conducting experiments. Ports are attached to both antennas. These antennas are placed in a box, which is assigned the properties of tissue material. Relative permittivity, electrical conductivity, and electrical loss tangent properties are defined as a function of frequency. Permeability and magnetic loss tangent are assigned frequency-independent and tissue-appropriate values [9]. Two simulations were carried out with probe separation distance of 30mm and 50mm respectively. Solutions were generated for frequencies ranging from 0.85GHz to 3GHz by using the interpolating-sweep method. Figures 3 and 4 compare the PMBA with HFSS results for separation distance 30mm and 50mm, respectively. HFSS results shows a maximum deviation of about 6dB at high frequencies when compared to PMBA. A slightly higher deviation of about 10dB is noticed in the case of 50mm separation distance. However, the results are encouraging since the rate of decrease is similar in both the cases. The deviation in the results can be attributed to the approximate SAR formula, which has a 3dB error margin, used in the derivation of CHMT and the use of numerical integration.

### B. Experiment

An experiment was conducted with Network Analyzer-HP 8510C at the Smart Advanced Antenna Lab, Arizona State University, for the validation of PMBA. Saturated salt solution was used as the medium between two probes (M/A-COM, Inc.) of Length 20mm and radius 0.5mm, in a non-reflecting thermal container. Saturated salt water was selected as a medium to make use of its well-known electrical properties and also because it has been used by many researchers for measurement of SAR and experimental verification purposes [15]. Proper precautions were taken in order to immerse the probes in the solution completely. Accuracy of maintaining distance between the probes was about  $\pm 1$ mm.

The experiment was aimed at plotting S-Parameters (specifically  $S_{21}$ ) for a range of frequencies from 900MHz to 3GHz.

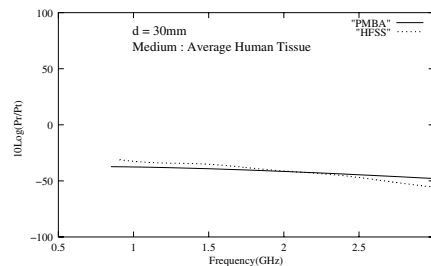


Fig. 3. Propagation loss computed by HFSS for tissue medium at d=30mm

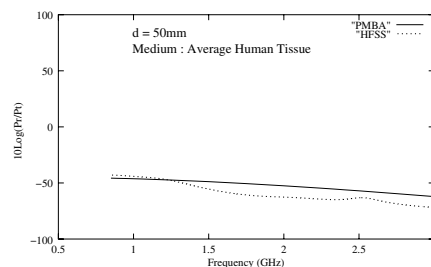


Fig. 4. Propagation loss computed by HFSS for tissue medium at d=50mm

Fig. 5 compares the loss predicted by PMBA with that computed by HFSS software and the experimental results for a separation distance of 30mm between the two probes. The HFSS model was simulated for saturated salt solution as a medium. The loss computed by PMBA increases consistently from about -54dB (at 900MHz) to about -61dB (3GHz) and the experimental value also increases in a similar fashion and comparable magnitude, but with a maximum fluctuation of 8dB in the values. This fluctuation is accounted for by experimental inaccuracies and reflections from imperfect absorbing materials around the experimental setup. However, the HFSS results shows about 10dB less loss throughout the frequency range. Reasons for this variation of HFSS results have been mentioned in the previous section. The experiment and analysis were repeated for various distances separating the two probes. In each case it is found that the propagation loss calculated from PMBA matches the propagation loss actually measured. Fig. 6 shows the comparison for a separation distance of 50mm between the probes. In this case, PMBA matches exactly with the HFSS simulations and also with the experimental results. Again the experimental inaccuracies lead to a maximum deviation of about 9dB.

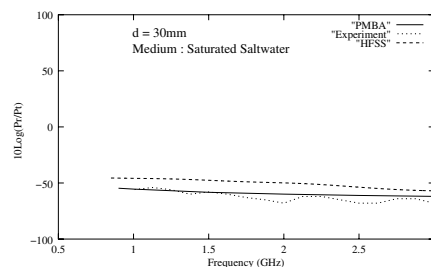


Fig. 5. Comparison of PMBA with Experimental results for d=30mm

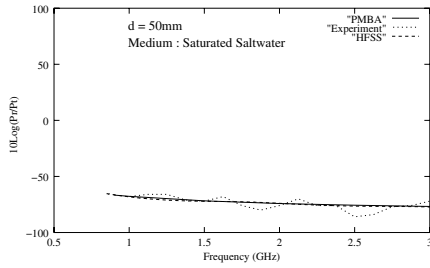


Fig. 6. Comparison of PMBA with Experimental results for  $d=50\text{mm}$

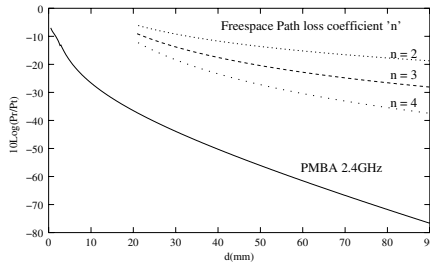


Fig. 7. PMBA (tissue medium) and Freespace Pathloss at 2.4GHz

## VI. CONCLUSIONS

In the case of fading channels in mobile communications, freespace formula is generally used with a higher loss coefficient (say  $n=3,4$ ). For estimating the propagation loss for wireless communications inside the human body, changing the loss coefficient only changes the rate of decrease in power, and does not help in estimating the total loss in the form of absorption. Fig. 7 compares PMBA with the freespace propagation model ( $P_R = P_T G_t G_r (\frac{\lambda}{4\pi d})^n$ ; with loss coefficients  $n=2,3,4$ ). It is observed that power received in PMBA decreases more rapidly than free-space pathloss ( $n=2,3,4$ ). Compared to freespace, there is an additional 30-35dB of attenuation at small distances in the far field. This loss increases further with the distance and frequency. It is noted from the simulation results that a major amount of power is absorbed in the near-field region of the antenna. Thus it cannot be ignored as in the case of other applications. It is clear that the amount of power absorbed (propagation loss) is more in the case of a medium with more water content. When substituted for properties of air (i.e., zero conductivity) in (5) and (6), the total loss involved in absorption of EM waves in near field and far field zones reduce to zero, resulting in the freespace formula. Thus the freespace propagation formula (Friis' Formula) can be viewed as a special case of PMBA.

There are many numerical techniques and experimental methods to estimate the EM wave power absorbed in the human body and are already explained in the related work section. However, a fixed model that can actually characterize the loss is not yet developed. Hence PMBA is one such model that is very useful in determining the loss of EM wave propagation in tissue. Verification of PMBA performed by HFSS simulations and measurements helps verify the formula. Though HFSS uses Maxwell's electromagnetic equations for lossy medium,

the loss predicted by PMBA was found to be in close agreement with those computed by HFSS software. In addition to it, the measurement results matches with PMBA. Thus PMBA paves the way toward the development of new upcoming wireless applications in lossy medium like human tissue involving communications between implantable devices within the human body [8][7][12]. It is important to note here that the derived formula holds good only in the case of a small dipole antenna. However, the power loss formula for similar applications with other antennas (e.g., microstrip) can be derived in a similar manner as described in Section IV.

In our future research, we plan to develop PMBA for a non-homogeneous medium, taking into consideration the reflection coefficients and correction factors. We also plan to refine our HFSS model and conduct experiments with real human tissue.

## VII. ACKNOWLEDGEMENTS

The authors would like to thank Mahmoud Zaghailil for his comments on an earlier version of the paper. This work is supported in part by NSF grant ANI-0086020.

## REFERENCES

- [1] T.S. Rappaport, "Wireless Communications, Principles and Practice", Prentice Hall, 1996.
- [2] C.A. Balanis, "Antenna Theory, Analysis and Design", Harper and Row, 1982.
- [3] David. K. Cheng "Field and Wave Electromagnetics" Addison-Wesley publications, Second Edition
- [4] "A Practical Guide to the Determination of Human Exposure to Radiofrequency Fields", NCRP Report No. 119, (1993)
- [5] Office of Engineering Technology "Understanding The FCC Regulations for Low-Power, Non-Licensed Transmitters" In OET BULLETIN NO. 63, Oct 1993.
- [6] Niels Kuster and Quirino Balzano "Energy Absorption Mechanism by Biological Bodies in the Near Field of Dipole Antennas Above 300 MHz", In IEEE Transactions on Vehicular Technology, Volume. 41, No. 1, February 1992.
- [7] V. Shankar, A. Natarajan, S.K.S. Gupta, L. Schwiebert, "Energy-efficient Protocols for Wireless Communication in Biosensor Networks", PIMRC 2001, in press.
- [8] L. Schwiebert, S.K.S. Gupta, P.S.G. Auner, G. Abrams, R. Lezzi, P. McAllister, "A Biomedical Smart Sensor for Visually Impaired", IEEE Sensors 2002, Orlando, FL, June 11-14
- [9] C. Gabriel, S. Gabriel "Compilation of the Dielectric Properties of Body Tissues at RF and Microwave Frequencies", June 1996, Report: Kings College London. <http://www.brooks.af.mil/AFRL/HED/hedr/reports/dielectric/home.html>
- [10] RF/Microwave Hazard Recognition and Measurement, <http://www.osha-slc.gov/SLTC/radiofrequencyradiation/rfpresentation/microwavemeasure/non2.html>
- [11] Dielectric Constant Reference Guide, <http://www.asiinstr.com/dc1.html>
- [12] C. Furse, H.K. Lai, C. Estes, A. Mahadik, A. Duncan, "An Implantable Antenna for Communication with Implantable Medical Devices", 1999, IEEE Antennas and Propagation/ URSI International Symposium, Orlando, FL
- [13] V.Pandit,R.McDermott,G.Lazzi,C.Furse,O.Gandhi, "Electrical Energy Absorption in the Human Head From a Cellular Telephone", 1996, IEEE International Symposium,
- [14] C.Furse,R.Mohan,A.Jakayar,S.Karidehal,B.McCleod,S.Going, "A Biocompatible Antenna for Communication with Implantable Medical Devices", 2001, IEEE International Symposium,
- [15] C.H. Durney, H. Massoudi, M.F. Iskander, "Radiofrequency Radiation Dosimetry Handbook, fourth edition", prepared for Amstrong laboratory (AFMC), October 1986 <http://www.brooks.af.mil/AFRL/HED/hedr/reports/handbook/tables.htm>